

Glass Bead Probes of Local Structural and Mechanical Properties of Fluid, Supported Membranes

Sanhita S. Dixit, Alan Szmodis, and Atul N. Parikh^{*[a]}

Nonspecific interactions between microscopic particles and a nearby “soft” surface report on the dynamical-mechanical properties of the surface. A realization of this principle is afforded by diverse systems exhibiting an interplay between energies of adhesion and local elastic deformation of the fluid.^[1,2] Within this framework, the behavior of supported, fluid lipid membranes interacting with microscopic colloids^[3] is particularly interesting because it offers a physical model for many biologically important mechanisms, such as particle engulfment, membrane fusion, and viral budding.^[3–6] Previous theoretical efforts establish that the elastic response of the membrane is determined by a finely coordinated balance between the adhesion, in-plane tension, and bending energies.^[7,8] Model experiments have focused primarily on the interaction between “free” membranes of giant phospholipid vesicles (>10 μm) and latex microspheres.^[9,10] Notable limitations of giant vesicles in modeling particle adhesion at biological membranes include their vanishingly low lateral tension and the presence of large, out-of-plane undulations.^[11,12] At cellular surfaces, however, the cytoskeleton constraints, the presence of transmembrane proteins, and even compositional asymmetries “re-normalize” membrane tension and limit the cooperativity in the natural dynamics of the two leaflets.^[13,14] In this regard, supported membranes provide an attractive model system.^[15,16] They are typically formed by rupture of lipid vesicles onto planar surfaces. Depending on the substrate’s hydrophilic or hydrophobic nature, vesicles rupture to form either bilayers or monolayers respectively.^[17] Bilayers are separated from the substrate surface by a thin water cushion ≈1–3 nm thick, which is believed to preserve their essential fluidity and their elastic structural properties.^[16,18] Lipid monolayers, on the other hand, experience a rigid hydrophobic interface with the substrate limiting the elastic response to a single leaflet. This provides a limiting case for decoupling of dynamics between the two membrane leaflets. In both cases, the lateral restrictions on membrane conformations imposed by the proximal

surface reduce the configurational entropy and increases lateral tension.

We presented microscopic, bare glass beads to binary patterns comprising alternate regions of 1) lipid bilayers and glass^[19] and 2) lipid monolayers and bilayers.^[17] Representative epifluorescence and brightfield data, shown in Figures 1 a and 1 b, display gravitationally settled beads on a patterned POPC (1-palmitoyl-2-oleoyl-*sn*-glycero-3-phosphocholine) bilayer (see Experimental Section). Beads settle uniformly over the entire surface. Physically perturbing the system via shaking or pipette pumping, selectively removes beads from the bare surface. Time-lapse bright-field images (Figures 1 b–1 f) reveal the formation of a visually striking patterned assembly of beads (a

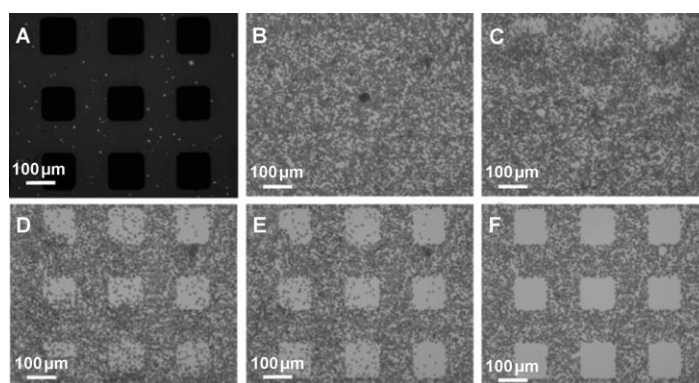


Figure 1. Amplification of bilayer patterns using beads. a) Epifluorescence and b) bright-field image of a patterned POPC bilayer doped with 1% Texas-Red DHPE with gravitationally settled 5.66 μm beads. The UV-generated glass voids are devoid of lipid and appear dark against a bright lipid grid. c)–f) Bead removal trajectory upon perturbation.

real-time movie is presented in Supporting Information, SI). A comparison with the epifluorescence image (Figure 1 a) of the underlying bilayer confirms a direct correspondence with the bead pattern (Figure 1 f).

This emergence of “epitaxial” bead patterns is understood in terms of differences in local interaction preferences. For membrane-voids, weight of the bead is balanced by the electrostatic repulsion from the planar glass substrate because of like negative charges.^[20,21] Indeed, we observe that glass beads hover over the exposed, lipid-free substrate regions executing the expected Brownian fluctuations with frustrated out-of-plane displacements.^[21] Thus, a small perturbation (e.g. shear) can displace the beads. By contrast, beads over the bilayer do not exhibit such Brownian dynamics due to a generic, but strong adhesive interaction between glass and the membrane. Previous studies have ascribed this interaction to a rather ill-understood combination of van der Waals, electrostatic, and hydration interactions.^[22]

Beads also settle uniformly on binary POPC patterns juxtaposing lipid bilayers (100×100 μm² squares) and surrounding single-leaflet lipid monolayers (Figure 2). As established previously, fluorescence emission from the bilayer is roughly twice as intense as the monolayer.^[17] Physically perturbing the

[a] Dr. S. S. Dixit, A. Szmodis, Prof. A. N. Parikh
Department of Applied Science and Biophysics Graduate Group
University of California, Davis, CA 95616 (USA)
Fax: (+1) 530-752-2444
E-mail: anparikh@ucdavis.edu

Supporting information for this article is available on the WWW under <http://www.chemphyschem.org> or from the author.

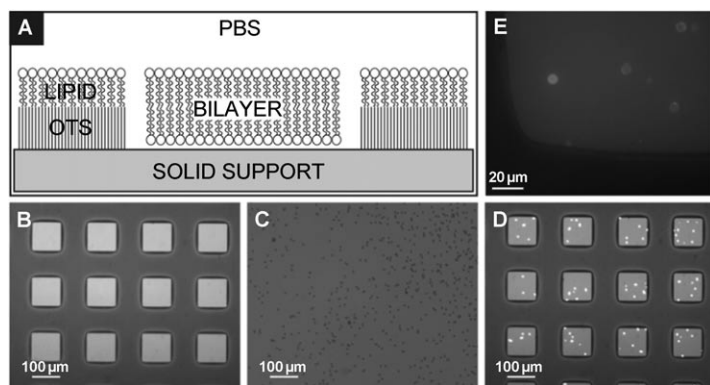


Figure 2. Discrimination of monolayer and bilayer morphologies using beads. a) A cartoon of the monolayer/bilayer lipid assembly on a patterned OTS substrate. b) Epifluorescence image of the sample prior to bead deposition. c) Brightfield and d) epifluorescence images showing 5.66 μm settled beads. Note that the beads in the bilayer region appear fluorescent. e) High magnification (60X, 0.63 NA) fluorescence image revealing membrane wrapping around the beads.

system, such as above, does not change the number of adherent beads on the monolayer or bilayer regions.

Epifluorescence images provide an additional contrast between the beads adhering to the bilayer and the monolayer regions. A fixed number of beads in the bilayer regions appear roughly four-times more fluorescent (Figures 2c and 2d), whereas beads on the monolayer region do not. The latter serves as a control negating possible lensing effects as cause for this increase in fluorescence intensity. Thus, this dramatic increase of fluorescence intensity reflects a significant wrapping of the beads by the underlying membrane bilayer.^[23] We note that a simple comparison of fluorescence intensity cannot be used to infer the extent of bead wrapping due to the changes in fluorescence emission at the perturbed membrane micro-environment in the vicinity of bead-bilayer interface. A rough calculation indicates $\approx 6\text{--}8\%$ expansion of the projected surface area due to membrane wrapping (see SI). Further, fluorescence recovery after photobleaching (FRAP) measurements in the vicinity of the fluorescent beads reveals two additional aspects of the colloid-membrane complex: 1) the lateral probe diffusivity of the membrane, a measure of membrane fluidity, appears to remain essentially unchanged before and after bead adhesion and 2) the membrane wrapped around the beads is essentially continuous with the underlying supported bilayer (see SI). In contrast, no such fluorescence acquisition by beads or membrane wrapping is seen in the monolayer regions. Taken together, these simple experiments suggest that the reversible adsorption of glass beads to fluid lipid membranes can be used as a simple means to differentiate local morphologies, namely, lipid bilayers from monolayers and voids or defects.

Next, we use the bead-membrane interaction to investigate how the lateral fluidity or phase state of the membrane influences its ability to deform following bead adhesion. We used binary monolayer/bilayer lipid patterns (see above) by spreading DMPC ($T_m = 24^\circ\text{C}$) vesicles at room temperature on a patterned OTS surface. The pattern is first cooled to 15°C . At this

temperature, FRAP measurements confirm the gel phase (Figure 3a) for the bilayer regions whereas the monolayer regions remain fluid. This apparently counter-intuitive monolayer fluidity parallels previous observations by Seul et al.^[24] where the melting of a monolayer depends on the properties of the underlying silane substrate. Sedimentation of glass beads on such a pattern, again, appears uniform. However, neither the gel bilayer (Figure 3b) nor the fluid monolayer of the pattern wet the beads. Upon heating the sample to 30°C , beyond the bilayer transition temperature, the beads adhering to bilayer regions selectively acquire fluorescence as seen in Figure 3c. The lipid monolayers, however, do not wrap around the beads. These results indicate that the binding to wrapping transition for bilayer-bead complex correspond well with the main phase transition of lipid bilayers and the onset of large-scale lateral fluidity in bilayers.^[25]

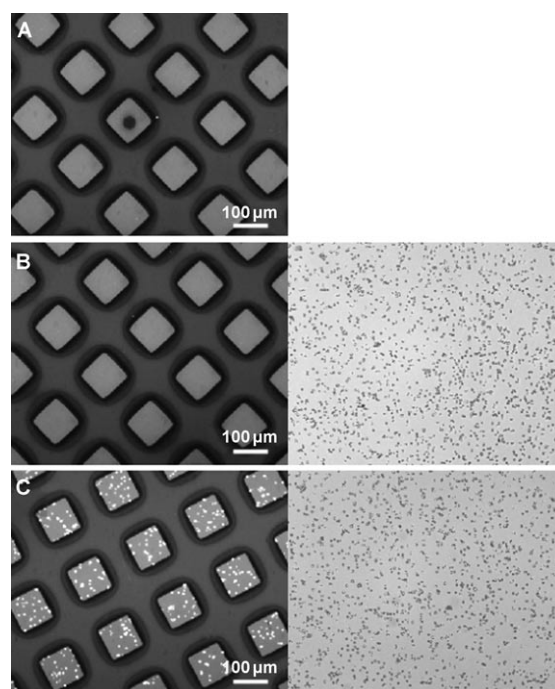


Figure 3. a) Fluorescence micrograph of DMPC monolayer/bilayer regions on a patterned OTS surface at 15°C . A photobleached spot at the center of the image does not recover in intensity and confirms the gel phase of the lipid bilayer. b) Fluorescence and brightfield images immediately after 5.66 μm bead sedimentation at 15°C . c) Fluorescent and brightfield images 15 min after heating the sample to 30°C shows fluorescent beads in the bilayer regions.

These qualitatively different responses to bead adhesion by symmetric bilayers and asymmetric, OTS supported lipid monolayers provide insights into elastic properties of supported membranes. First, for lipid monolayers supported on OTS, the lower leaflet equivalent, namely OTS, is directly tethered to the substrate. As a result, the “unbinding” of lipid monolayers required to wrap around the beads must impose a high hydro-

phobic penalty through the requisite separation at the hydrophobic mid-plane and is therefore expected to be strongly suppressed. Our results are entirely consistent with this picture and provide a practical caveat against direct comparisons of adhesive responses of monolayer and bilayer based models. They further suggest that the interactions between the inner leaflet of biological membranes and cytoskeleton may modulate the membrane's elastic response to local deformation. Second, the response of the lipid bilayer, namely wrapping, sandwiched between the flat and the curved adhesive substrates can be understood in terms of the interplay between adhesion, bending, and tension energies.^[7,26] The presentation of the bead provides a new source of adhesion energy for the membrane. The contact energy of adhesion^[27] with beads ($= -k_{\text{ad}} A_{\text{ad}} = k_{\text{ad}} 2\pi a^2 z$ where z is the extent of membrane wrapping in the units of the colloidal radius a and k_{ad} represents the adhesion constant) drives the membrane assembly around the beads. In the limiting case, if the bead-membrane adhesion energy exceeds substrate-membrane adhesion energy substantially,^[8] the parent bilayer unbinds from the planar glass wrapping the contacting beads. In our case, the bead-membrane and substrate-membrane interactions share comparable (glass-lipid) physical-chemical interactions resulting in an elastic membrane deformation.

The nature of this local membrane deformation is understood as a result of the competing interactions due to the tension ($= \pi a z 2z \sigma$ where σ is the lateral tension within the membrane) and curvature energies ($= 1/2 k (C_1 + C_2)^2 A_{\text{ad}} = 4\pi z k$ where k is bending constant) of the membrane^[27] under the constraints of planar membrane configuration. As the characteristic length scale for the bending energy for fluid bilayers^[3] [$= (k/\sigma)^{1/2} \sim 10\text{--}50\text{ nm}$] is much smaller than the bead dimensions used, the observed wrapping or membrane area dilation must result in a corresponding rise in tension energy due to the membrane's elastic area compressibility. By accounting for the number of fluorescent beads per membrane area and near-complete wrapping of the beads by the membrane in Figure 2 and related controls (see SI), we estimate the membrane stretching to be roughly 6–8% in our data. This area dilation is accounted for by a combination of the membrane excess stored in the thermal undulations of the supported bilayer and an increase in the average separation between neighbouring lipids above its optimal value. The latter type of area expansion involves a significant hydrophobic penalty and is limited to 2–4% before membrane rupture or lysis and the loss of planar topology.^[11] The former is attributed to thermally excited undulations ascribed previously to thickness and relative tilt variation modes^[28] which are preserved in fluid supported membranes.^[8] Additional support for this tension-induced area dilation explanation is provided by our observations that below the transition temperature, DMPC bilayers do not wrap around the beads. The elastic area compressibilities of "free" DMPC bilayers have been previously shown to decrease by an order of magnitude (lateral compressibility modulus decreases from 50–60 dyne cm^{-1} for L_{α} fluid phase to almost 1000 dyne cm^{-1} for the solid L_{β} phase).^[29] Thus, in principle, by simply allowing the beads of known physical proper-

ties (e.g. weight and charge) to settle on supported membranes, local tension, area dilation, and hence its elastic area compressibility are determined. Such experiments require precise determination of the extent of membrane wrapping. High-resolution fluorescence microscopy and total internal reflection fluorescence^[20] investigations are in progress in our laboratory to achieve such quantitative determinations. We note that existing methods for such measurements, namely micro-pipette aspiration^[30] and physical compression^[31] are not easily amenable to the planar supported membrane configuration.

In summary, interactions between glass beads and supported lipid membranes can be used as a simple tool to characterize their local structural and mechanical properties. The affinity difference of the beads for bilayers and glass results in a 100- to 500-fold amplification of the underlying membrane patterns and void-defects producing optical contrasts. Beads differentiate monolayers from fluid bilayers by inducing a qualitatively different elastic response, characterized by non-wetting or non-deformed binding for monolayers and partial wetting or membrane wrapping for bilayers. These results confirm the essential role of inter-leaflet coupling and bilayer fluidity in determining elastic response of supported membranes.

Experimental Section

Membrane patterns were produced following membrane photolithography methods.^[17,19] Briefly, a supported bilayer on coverglass was exposed to short-wavelength UV-radiation in an aqueous environment through a physical mask to produce well-defined voids in the bilayer reflecting the pattern of the lithographic mask (Figure 1a). A dry version of this patterning technique was used to generate micrometer scale patterns of hydrophilic voids in octadecyltrichlorosilane (OTS) coated glass coverslips. Spreading of phospholipid vesicles on a patterned OTS surface resulted in the formation of lipid monolayers on the OTS grid and lipid bilayers in the UV-generated voids.

Phospholipids used were 1-palmitoyl-2-oleoyl-*sn*-glycero-3-phosphocholine (POPC) and 1,2-dimyristoyl-*sn*-glycero-3-phosphocholine (DMPC, Avanti) Small unilamellar vesicles (SUVs) were prepared from hydrated multilamellar lipid stock solution following the extrusion method. The SUVs were doped with 1 mol% Texas Red 1,2-dihexadecanoyl-*sn*-glycero-3-phosphoethanolamine, triethylammonium salt (TR-DHPE, Molecular Probes) to enable visualization by fluorescence. Glass coverslips (Corning) were oxidized using Piranha etch solution (3:1, sulfuric acid: hydrogen peroxide, 5 min, 90 °C). All experiments occurred in PBS (phosphate buffer saline, pH 7.4, 137 mM NaCl, 2.7 mM KCl). Glass beads (diameter $5.66 \pm 0.76\ \mu\text{m}$ and $0.97 \pm 0.10\ \mu\text{m}$; 2.2 g ml^{-1} ; 10% in DI water, Bangs Labs), diluted 100-fold in PBS, were incubated with patterned lipidic surfaces placed at the bottom of crystallization wells. Under these conditions, all bare glass surfaces display a net negative charge via dissolution of surface silanol groups.^[32] Microscopy images were acquired using a Nikon eclipse TE2000-S microscope equipped with fluorescence and brightfield capabilities.

Acknowledgements

We thank A. Boulbitch, G. Swadener, J. Groves, and N. Banerjee for useful suggestions. We are supported by DOE (DE-FG02-

04ER46173), NSF Center for Biophotonics, and NIH Graduate Fellowship for AWS (NIGMS 1-T32-GM08799).

Keywords: fluorescence · interfaces · membranes · monolayers · phospholipids

- [1] H. Hertz, *Miscellaneous Papers*, McMillan, London, **1896**.
- [2] B. N. J. Persson, F. Mugele, *J. Phys. Condens. Matter* **2004**, *16*, R295.
- [3] M. Deserno, *J. Phys. Condens. Matter* **2004**, *16*, S2061.
- [4] J. Zimmerberg, L. V. Chernomordik, *Adv. Drug Delivery Rev.* **1999**, *38*, 197.
- [5] F. S. Cohen, G. B. Melikyan, *J. Membr. Biol.* **2004**, *199*, 1.
- [6] H. Garoff, R. Hewson, D. J. E. Opstelten, *Microbiol. Mol. Biol. Rev.* **1998**, *62*, 1171.
- [7] A. Boulbitch, *Europhys. Lett.* **2002**, *59*, 910.
- [8] C. Tordeux, J. B. Fournier, *Langmuir* **2000**, *16*, 2991.
- [9] I. Koltover, J. O. Radler, C. R. Safinya, *Phys. Rev. Lett.* **1999**, *82*, 1991.
- [10] C. Dietrich, M. Angelova, B. Pouligny, *J. Phys. II* **1997**, *7*, 1651.
- [11] U. Seifert, *Adv. Phys.* **1997**, *46*, 13.
- [12] M. B. Schneider, J. T. Jenkins, W. W. Webb, *J. Phys.* **1984**, *45*, 1457.
- [13] P. Girard, J. Prost, P. Bassereau, *Phys. Rev. Lett.* **2005**, *94*.
- [14] J. D. Cortese, B. Schwab, C. Frieden, E. L. Elson, *Proc. Natl. Acad. Sci. USA* **1989**, *86*, 5773.
- [15] E. Sackmann, *Science* **1996**, *271*, 43.
- [16] S. G. Boxer, *Curr. Opin. Chem. Biol.* **2000**, *4*, 704.
- [17] M. C. Howland, A. R. Sapuri-Butti, S. S. Dixit, A. M. Dattelbaum, A. P. Shreve, A. N. Parikh, *J. Am. Chem. Soc.* **2005**, *127*, 6752.
- [18] S. Y. Bhide, M. L. Berkowitz, *J. Chem. Phys.* **2005**, *123*.
- [19] C. K. Yee, M. L. Amweg, A. N. Parikh, *Adv. Mater.* **2004**, *16*, 1184.
- [20] D. C. Prieve, *Adv. Colloid Interface Sci.* **1999**, *82*, 93.
- [21] S. H. Behrens, D. G. Grier, *Phys. Rev. E* **2001**, *6405*.
- [22] P. S. Cremer, S. G. Boxer, *J. Phys. Chem. B* **1999**, *103*, 2554.
- [23] M. Deserno, T. Bickel, *Europhys. Lett.* **2003**, *62*, 767.
- [24] M. Seul, S. Subramaniam, H. M. McConnell, *J. Phys. Chem.* **1985**, *89*, 3592.
- [25] T. Heimburg, *Biochim. Biophys. Acta* **1998**, *1415*, 147.
- [26] M. Deserno, *Phys. Rev. E* **2004**, *69*.
- [27] M. Deserno, W. M. Gelbart, *J. Phys. Chem. B* **2002**, *106*, 5543.
- [28] M. Hamm, M. M. Kozlov, *Eur. Phys. J. E* **2000**, *1*, 323.
- [29] E. Evans, D. Needham, *J. Phys. Chem.* **1987**, *91*, 4219.
- [30] E. Evans, R. Kwok, *Biochemistry* **1982**, *21*, 4874.
- [31] V. A. Parsegian, N. Fuller, R. P. Rand, *Proc. Natl. Acad. Sci. USA* **1979**, *76*, 2750.
- [32] S. H. Behrens, D. G. Grier, *J. Chem. Phys.* **2001**, *115*, 6716.

Received: April 9, 2006

Published online on July 17, 2006